Advanced Topics in Chemical Physics

Adam Kirrander*
School of Chemistry, University of Edinburgh, David Brewster Road, Edinburgh EH9 3FJ, United Kingdom
(Dated: January 24, 2018)

Reading notes for Part 1 (Theory) for the *Advanced Topics in Chemical Physics* lecture course in Year 4-5.

* Adam.Kirrander@ed.ac.uk

CONTENTS

I. DYNAMICS

A. Why bother with the time-dependent Schrödinger equation?

For a long time the prevailing attitude was that time-independent quantum mechanics was sufficient to understand any dynamic process involving atoms and molecules, and little attention was given to time-dependent quantum mechanics. Indeed, if the Hamiltonian describing the system is time-independent, the normal scenario for atoms and molecules, all available information can be garnered from solving the time-independent Schrödinger equation. For instance, in the 1970s molecular beam and crossed-beam experiments tremendously advanced our understanding of chemical reaction dynamics [1], but only required time-independent quantum mechanics for analysis and interpretation [2]. Of course, some physical phenomena, such as electromagnetic fields, are inherently time-dependent, but such phenomena were treated in their capacity to transfer the atom or molecule from one set of stationary eigenstates to another. Phenomena such as electromagnetic fields (light) simply provided the perturbation necessary to excite and probe various eigenstates of the system, and once time-dependent perturbation theory had been used to calculate the appropriate transition matrix elements (and for symmetric systems appropriate selection rules had been derived), one could forget all about time-dependence and dynamics.

Since the 1980s the time-dependent Schrödinger equation (TD-SE) has increasingly come into focus. There are four main reasons for this. First, theoreticians such as Eric Heller at Harvard University realized in the late 1970s and early 1980s that solving the TD-SE could provide an efficient route to the calculation of the spectra of (larger) molecules [3]. Second, rapid developments in laser technology have provided experimentalists with the tool to routinely make time-dependent measurements with picosecond (ps), femtosecond (fs), or even attosecond (as) time-resolution, putting dynamics into focus. Importantly, due to the short duration and coherence of the laser pulses, a non-stationary wavepacket is invariably excited in these experiments. Third, using modern laser technology, it has become possible to focus light to intensities which are non-perturbative, meaning that the Hamiltonian is inseparably time-dependent. As a consequence such experiments must be described by solving the full time-dependent Schrödinger equation. Fourth, there is a strong belief that time-dependent calculations and measurements yield more intuitive insight into dynamic transformations of matter, including reaction mechanisms.

B. The time-dependent Schrödinger equation

Recall the time-independent Schrödinger equation (SE),

$$H_0|i\rangle = E_i|i\rangle, \tag{1}$$

where H_0 is the field-free, time-independent, molecular or atomic Hamiltonian (consisting of an operator representation of kinetic and potential energies), $|i\rangle$ is the normalized eigenstate, and E_i is the corresponding energy of the eigenstate. The SE is a differential eigenvalue equation that can be solved analytically in simple cases (essentially one-dimensional problems such as the particle-in-the-box, the harmonic oscillator, the H-atom, H_2^+, and some other examples) while more generally must be solved using numerical methods that use a discrete space representation (grid) or basis functions [4]. The full set of solutions to Eq. (1) forms a complete set, $\mathbb{1} = \sum_i |i\rangle\langle i|$, where $\mathbb{1}$ is the identity operator. For bound potentials, physically meaningful solutions exist only at specific energies, while for unbound potentials solutions exist over a continuous range of E. We refer to the energies corresponding to valid solutions as the "spectrum".

The time-dependent Schrödinger equation provides the evolution, i.e. *dynamics*, of any quantum system, for instance an atom or molecule. It is given by,

$$\imath\hbar\frac{\partial|\Psi\rangle}{\partial t} = H_0|\Psi\rangle, \tag{2}$$

where $\imath = \sqrt{-1}$, $\hbar = h/2\pi$ (h is Planck's constant), and H_0 the same molecular or atomic Hamiltonian as in Eq. (1) above. The TD-SE can be solved numerically given an initial solution that is then propagated in time [5]. The relationship between the time-independent and time-dependent Schrödinger equations yields physical and mathematical insight. For a Hamiltonian H_0 that is independent of time, we can solve the TD-SE in Eq. (2) using separation of variables with the ansatz $\Psi(\mathbf{x}, t) = \chi(t)\psi(\mathbf{x})$. Substituting into Eq. (2) and dividing both sides by $\chi(t)\psi(\mathbf{x})$ yields,

$$\imath\hbar\frac{\dot{\chi}(t)}{\chi(t)} = \frac{H_0\psi(\mathbf{x})}{\psi(\mathbf{x})}. \tag{3}$$

The left-hand side of Eq. (3) is a function of time, while the right-hand side is a function of coordinates $\mathbf{x}$. For equality, both sides must be equal to a constant, which we call E (you may convince yourself via dimensional analysis that the constant E must

have units of energy). We then obtain two equations, one for $\psi(\mathbf{x})$ and one for $\chi(t)$:

$$\imath\hbar\dot{\chi}(t) = E\chi(t) \tag{4}$$
$$H_0\psi(\mathbf{x}) = E\psi(\mathbf{x}), \tag{5}$$

where Eq. (5) is the already familiar time-independent Schrödinger equation (SE) presented in Eq. (1), while solutions to Eq. (4) are given by,

$$\chi(t) = \chi_0 e^{-\imath Et/\hbar}. \tag{6}$$

The overall solution to the TD-SE can therefore be written as

$$|\Psi(\mathbf{x},t)\rangle = \psi(\mathbf{x})e^{-\imath Et/\hbar}, \tag{7}$$

where the constant χ_0 has been absorbed by $\psi(\mathbf{x})$ under the condition that the function is normalised,

$$1 = \int |\Psi(\mathbf{x},t)|^2 \, d\mathbf{x} = \int |\psi(\mathbf{x})|^2 \, d\mathbf{x}. \tag{8}$$

Note that the solution has a rather trivial time-dependence, since the stationary solution simply rotates in the complex plane according to a time-dependent phase factor, which has no physical manifestation. For instance, if we consider the probability density $|\Psi(\mathbf{x},t)|^2$ of the wavefunction in Eq. (7) we obtain,

$$|\Psi(\mathbf{x},t)|^2 = \left(\psi(\mathbf{x})e^{-\imath Et/\hbar}\right)^* \left(\psi(\mathbf{x})e^{-\imath Et/\hbar}\right) = |\psi(\mathbf{x})|^2, \tag{9}$$

which is independent of time t. Since the TDSE is a linear differential equation, a general solution $|\Psi\rangle$ to the TD-SE can be written as a linear expansion of solutions,

$$|\Psi\rangle = \sum_i c_i e^{-\imath\omega_i t}|i\rangle, \tag{10}$$

where c_i are expansion coefficients corresponding to the problem at hand, $|i\rangle$ are eigenstates of the corresponding time-independent Schrödinger equation, and the phase factors depend on $\omega_i = E_i/\hbar$, with ω_i the angular frequency. The expression in Eq. (10) is a solution to the TD-SE equation known as a wavepacket, written as a coherent, non-stationary superposition of time-independent eigenstates $\{|i\rangle\}$.

It is straightforward to show that the norm of the wavepacket $|\Psi\rangle$ is conserved,

$$1 = \langle\Psi|\Psi\rangle = \sum |c_i|^2, \tag{11}$$

using the orthonormality of the stationary solutions (Problem III 2). However, in contrast to a stationary state which has a static probability distribution $\rho(\mathbf{x}') = |\langle\mathbf{x}'|i\rangle|^2$, the probability distribution associated with a wavepacket is time-dependent,

$$\rho(\mathbf{x}',t) = |\langle\mathbf{x}'|\Psi\rangle|^2 = \sum_i |c_i|^2|\langle\mathbf{x}'|i\rangle|^2 + \sum_{i\neq j} c_i^* c_j \langle i|\mathbf{x}'\rangle\langle\mathbf{x}'|j\rangle e^{\imath\omega_{ij}t} = \sum_i |c_i|^2|\langle\mathbf{x}'|i\rangle|^2 + \sum_{i>j} 2\Re\left\{c_i^* c_j \langle i|\mathbf{x}'\rangle\langle\mathbf{x}'|j\rangle e^{\imath\omega_{ij}t}\right\}, \tag{12}$$

where $\omega_{ij} = \omega_i - \omega_j$. In Eq. (12) we see dynamics emerge as an interference phenomenon, a theme that resonanates throughout quantum mechanics.

C. Example: A two-state wavepacket

Lets first examine the simple case of a two-state wavepacket, using the coordinate representation for the wavefunctions and assuming that the wavefunctions $\phi_1(x)$ and $\phi_2(x)$ are real-valued with the expansion coefficients $c_1 = c_2 = 1/\sqrt{2}$,

$$\Psi(x,t) = \frac{1}{\sqrt{2}}\phi_1(x)e^{-\imath\omega_1 t} + \frac{1}{\sqrt{2}}\phi_2(x)e^{-\imath\omega_2 t}. \tag{13}$$

The corresponding probability distribution is,

$$|\Psi(x,t)|^2 = \frac{1}{2}\left[|\phi_1(x)|^2 + |\phi_2(x)|^2 + 2\phi_1(x)\phi_2(x)\cos\omega_{12}t\right], \tag{14}$$

where the final term gives rise to the interference and thus time-dependence. In this particular scenario, the wavepacket dynamics has a period of $T = 2\pi/\omega_{12}$ corresponding to the time it takes for the wavepacket to repeat itself. In fact, bound quantum systems will always display periodicity, at least in principle, and the link between quantum periodicity and classical chaos is a topic that has been studied extensively.

The expectation value of an observable A corresponding to the operator $\hat{A}$ is,

$$\langle A(t)\rangle = \langle\Psi(x,t)|\hat{A}|\Psi(x,t)\rangle. \tag{15}$$

which in contrast to the expectation values for stationary states, *does* depend on time. To take a simple example, the expectation value of the position x of the wavepacket is,

$$\langle x(t)\rangle = \frac{1}{2}\left[\int x|\phi_1(x)|^2\,dx + \int x|\phi_2(x)|^2\,dx + 2\int x\phi_1(x)\phi_2(x)\cos\omega_{12}t\,dx\right], \tag{16}$$

with the time-dependence provided, again, by the final term corresponding to interference between the two stationary states.

D. Example: Particle in a box

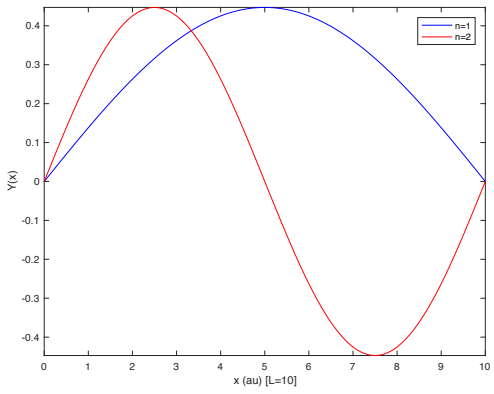

FIG. 1: Particle in a box wavefunctions for $n = 1$ and $n = 2$ in box with $L = 10$ a_0.

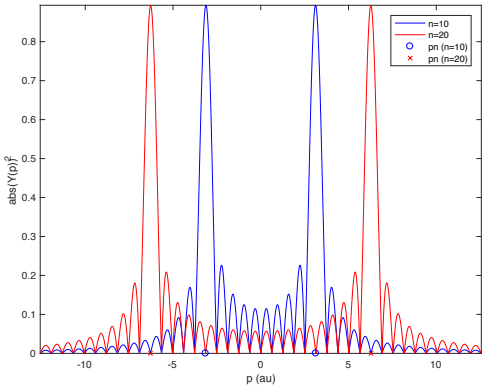

FIG. 2: Probability amplitude for particle in a box wavefunctions in momentum representation for $n = 10$ and $n = 20$ in box with $L = 10$ a_0.

1. *Basic solution*

The particle in a box is one of the simplest quantum mechanical problems. The Hamiltonian is,

$$H_0 = -\frac{\hbar^2}{2m}\frac{d^2}{dx^2} + V(x), \quad V(x) = \begin{cases} 0, & 0 < x < L \\ \infty, & x \leq 0, x \geq L \end{cases}, \tag{17}$$

with L the length of the box. The solutions can be written as either $\Psi(x) = A'e^{\imath kx} + B'e^{-\imath kx}$ or $\Psi(x) = A\cos kx + B\sin kx$, with the energy $E = \frac{\hbar^2 k^2}{2m}$ (purely kinetic in this case). It is convenient to enforce the required boundary conditions using the real-valued solution:

$$\Psi(x = 0) = 0 \Rightarrow B = 0$$
$$\Psi(x = L) = 0 \Rightarrow k_n = \pi n/L, \tag{18}$$
$$\tag{19}$$

which results in the quantized energies E_n,

$$E_n = \frac{\hbar^2\pi^2 n^2}{2mL^2} = \frac{h^2 n^2}{8mL^2}. \tag{20}$$

The constant A is determined via the normalization condition,

$$1 = \int_0^L \sin^2\frac{\pi nx}{L}\,dx = \int_0^L \frac{1}{2}\left(1 - \cos\frac{2\pi nx}{L}\right)dx = \frac{L}{2} \quad \Rightarrow \quad A = \sqrt{\frac{2}{L}}. \tag{21}$$

These results give the wavefunctions as,

$$\Psi_n(x) = \sqrt{\frac{2}{L}} \sin \frac{\pi n x}{L}. \tag{22}$$

The corresponding momentum wavefunction $\tilde{\Psi}_n(p)$ is the Fourier transform of the position wavefunction $\Psi_n(x)$,

$$\tilde{\Psi}_n(p) = \frac{1}{\sqrt{2\pi\hbar}} \int_{-\infty}^{\infty} \Psi_n(x) e^{-\imath p x/\hbar}\, dx = \sqrt{\frac{\hbar}{\pi L}} \left(\frac{p_n}{p_n^2 - p^2} \right) \left[1 - (-1)^n e^{-\imath p L/\hbar} \right], \tag{23}$$

with the momentum distribution centered on p_n as expected (Problem III 3). Coordinate representation wavefunctions for $n = 1, 2$ are shown in Fig. 1, and the probability amplitude for momentum representation particle in a box wavefunctions for $n = 10, 20$ are shown in Fig. 2.

2. *β-carotene*

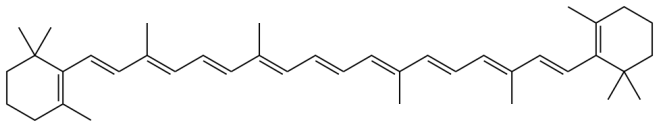

FIG. 3: The conjugated polyene β-carotene $C_{40}H_{56}$ with 11 double bonds and 22 π-electrons. The molecule has an approximate length of 3.8 nm (2.4 nm chain length).

The particle in the box can be used as a approximate model of the conjugated polyene β-carotene $C_{40}H_{56}$ shown in Fig. 3, which has 11 double bonds and 22 π-electrons. The molecule has an approximate length of 3.8 nm (2.4 nm chain length) and the mass of an electron is 9.109×10^{-31} kg. From Eq. (20) the transition energies are given by

$$\triangle E_{fi} = \frac{(n_f^2 - n_i^2)h^2}{8mL^2}. \tag{24}$$

The HOMO is $n = 11$ and the LUMO $n = 12$, giving the excitation (absorption) energy as 2.3658×10^{-19} J for $11 \rightarrow 12$. Using the $\lambda = \frac{hc}{\triangle E}$ relationship, we get an absorption wavelength of 840 nm. The actual absorption maximum is 450 nm - not bad for such a simple model.

3. *Wavepacket*

Now consider that the molecule is excited by a pulse with sufficient bandwidth to excite LUMO + (LUMO+1), i.e. states $n = 12$ and $n = 13$. The wavepacket is (assuming both states are excited equally with the same phase),

$$\Psi(x,t) = \frac{1}{\sqrt{2}} \Psi_{12}(x) e^{-\imath E_{12} t/\hbar} + \frac{1}{\sqrt{2}} \Psi_{13}(x) e^{-\imath E_{13} t/\hbar}, \tag{25}$$

with corresponding probability density given by Eq. (14). In contrast to stationary wavefunctions, the probability distribution clearly changes with time - this is a nonstationary state. Snapshots of the dynamics is shown in Fig. 4 at times t corresponding to fractions $0, T/4, T/2$ of the period $T = 2\pi/\triangle\omega_{13,12}$. At time $t = T$ the wavepacket undergoes what is known as a full revival: it returns to its original $t = 0$ form. More complicated wavepackets may also exhibit partial revivals known as fractional revivals - in time-dependent spectroscopy revivals appear as so-called beats. Finally it is instructive to examine the probability flux associated with the wavepacket in Fig. 4. The flux at $x = L/2$ is shown in Fig. 5 for a a full period ($t \in [0, T]$. We can clearly see how the probability density (and thus the particle) oscillate back and forth.

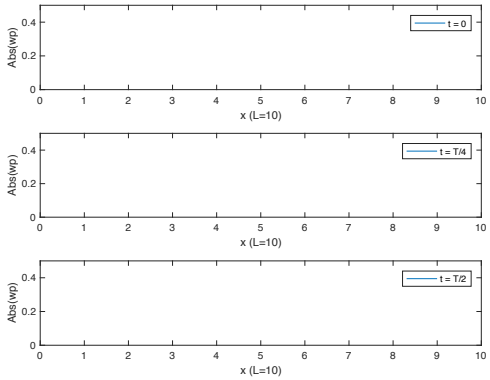

FIG. 4: Probability amplitude for particle in a box wavepacket using only two states $n = 12$ and $n = 13$ with expansion coefficients $2^{-1/2}$ plotted at times $t = 0, T/4, T/2$ (from top to bottom) with $T = 2\pi/\Delta\omega$ is the classical period. In this particular example the length of the box is $L = 10$ a_0.

E. Example: Free particle

1. *Basic solution*

The Hamiltonian for a free particle is simply the kinetic energy operator,

$$H_0 = -\frac{\hbar^2}{2m}\frac{d^2}{dx^2}, \tag{26}$$

with solutions,

$$\Psi(x) = \frac{1}{\sqrt{2\pi\hbar}} e^{\pm \imath p' x/\hbar}. \tag{27}$$

The solutions are not quantized, since this is a continuum (unbound) problem. Therefore the standard normalisation condition does not apply (try it - the solutions are not normalisable to 1). Instead one uses momentum, $\delta(p - p')$, or energy, $\delta(E - E')$, normalisation, where $\delta(x)$ is the delta function. The wavefunctions in Eq. (133) are momentum normalised. We see this normalisation in action if we determine the momentum space form, $\tilde{\Psi}(p)$, of the free-particle wavefunction, $\Psi(x) = (2\pi\hbar)^{-1/2} e^{\imath p' x/\hbar}$,

$$\tilde{\Psi}(p) = \frac{1}{\sqrt{2\pi\hbar}} \int_{-\infty}^{\infty} \Psi(x) e^{-\imath p x/\hbar}\, dx = \frac{1}{2\pi\hbar} \int_{-\infty}^{\infty} e^{-\imath (p'-p) x/\hbar}\, dx = \delta(p - p'), \tag{28}$$

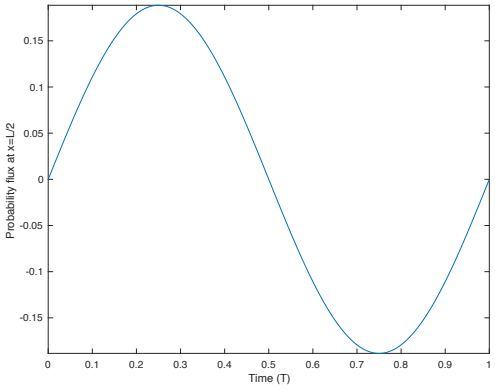

FIG. 5: Flux as a function of time for particle in a box wavepacket calculated at $x = L/2$ where $L = 10$ a_0 is the length of the box. The wavepacket consists of two states $n = 12$ and $n = 13$ with expansion coefficients $2^{-1/2}$, and the range of time is $0 < t < T$, where $T = 2\pi/\Delta\omega$ is the classical period.

which unsurprisingly corresponds to a single (normalised) point in momentum space. The energies of the Hamiltonian are,

$$E = \frac{p^2}{2m} = \frac{\hbar^2 k^2}{2m}, \tag{29}$$

where $k = p/\hbar$ is the wavenumber with $k\lambda = 2\pi$ (i.e the de Broglie relation $p\lambda = h$). In multidimensional scenarios we must consider the wavevector $\mathbf{k}$ instead, with $|\mathbf{k}| = k$.

2. *Wavepacket*

We can define a wavepacket in complete analogy with Eq. (10),

$$\Psi(x,t) = \int_{-\infty}^{\infty} c(p')\Psi(x)e^{-\imath\omega t}\, dp', \tag{30}$$

where $\omega = E/\hbar = \hbar k^2/2m$. Since we are dealing with a continuum wavepacket, $c(p)$ is an arbitrary continuous function of the momentum p, instead of a set of discrete expansion coefficients $\{c_i\}$ as in Eq. (10). The corresponding momentum-space

representation of the wavepacket in Eq. (30) is,

$$\tilde{\Psi}(p,t) = \frac{1}{\sqrt{2\pi\hbar}} \int_{-\infty}^{\infty} \Psi(x,t) e^{-\imath px/\hbar}\, dx \tag{31}$$

$$= \int_{-\infty}^{\infty} c(p') e^{-\imath\omega t} \left[\frac{\int_{-\infty}^{\infty} e^{-\imath(p'-p)x/\hbar}\, dx}{2\pi\hbar} \right] dp', \tag{32}$$

$$= \int_{-\infty}^{\infty} c(p') e^{-\imath\omega t} \delta(p-p')\, dp', \tag{33}$$

$$= c(p) e^{-\imath\omega t}, \tag{34}$$

where it is apparent that the distribution in momentum is independent of time $|\tilde{\Psi}(p,t)|^2 = |c(p)|^2$, which is to be expected since there is no potential that acts on the free particle. It is straightforward to show that if the coordinate-space wavepacket is normalised, then the momentum-space wavepacket is too (Problem III 4).

3. *Center of wavepacket*

We now consider the time evolution of the center of the normalised wavepacket, $\Psi^*(x,t)$,

$$\langle x \rangle_t = \int_{-\infty}^{\infty} \Psi^*(x,t)\, x\, \Psi^*(x,t)\, dx, \tag{35}$$

where the subscript t reminds us that the expectation value $\langle x \rangle$ is time-dependent. The evaluation of this integral can be done analytically in the momentum representation, using the fact that the $\hat{x}$ operator is given by $\imath\hbar\partial/\partial p$ in momentum representation,

$$\langle x \rangle_t = \int_{-\infty}^{\infty} c^*(p) e^{\imath\omega t} \imath\hbar \frac{\partial}{\partial p} c(p) e^{-\imath\omega t}\, dp, \tag{36}$$

$$= \int_{-\infty}^{\infty} c^*(p) \imath\hbar \frac{\partial}{\partial p} c(p) + c^*(p) c(p) e^{\imath\omega t} \imath\hbar \frac{\partial}{\partial p} e^{-\imath\omega t}\, dp \tag{37}$$

$$= \int_{-\infty}^{\infty} c^*(p) \imath\hbar \frac{\partial}{\partial p} c(p)\, dp + \int_{-\infty}^{\infty} |c(p)|^2 \frac{pt}{m}\, dp \tag{38}$$

$$= \langle x \rangle_0 + \frac{p}{m} \int_{-\infty}^{\infty} |c(p)|^2 t\, dp \tag{39}$$

$$= \langle x \rangle_0 + \frac{\langle p \rangle}{m} t, \tag{40}$$

where we used that $\omega = p^2/2m\hbar$, and have simply identified the time-independent integral (the one on the left) as the constant term $\langle x \rangle_0$, while inspection of the second integral allows us to identify $\langle p \rangle$. Notably, the resulting expression agrees with propagation of a particle in classical mechanics! We can define the group velocity, v_g, as the velocity of the center of the wavepacket,

$$v_g = \frac{d\langle x \rangle_t}{dt} = \frac{\langle p \rangle}{m}, \tag{41}$$

which is the direct analogue of the classical relation $v_{cl} = p_{cl}/m$. For a free particle the group velocity is independent of time, as in classical mechanics, and is completely determined by the distribution $c(p)$. It is also worth noting that the result is congruent with general wavemechanics which gives the group velocity as,

$$v_g = \langle \frac{\partial \omega}{\partial k} \rangle = langle \frac{\hbar k}{m} \rangle = \frac{\langle p \rangle}{m}, \tag{42}$$

where we have used that $\omega = \hbar k^2/2m$. This result is consistent with the result we obtain above, as expected.

4. Dispersion of wavepacket

The width of a wavepacket can be calculated using the variance,

$$\mathrm{Var}(x) = \triangle x^2 = \langle x^2 \rangle - \langle x \rangle^2, \tag{43}$$

where the mean deviation, $\triangle x$, is a measure of the width. The width of wavepackets has a tendency to increase as the wavepacket disperses, especially in for instance photochemistry, where the pump laser has a tendency to prepare rather localised wavepackets via vertical excitation from the generally compact initial state. The increase of the width with time is known as dispersion, and we will examine the dispersion (related to the time-dependence of the variance) for the case of a free particle wavepacket.

We have already calculated $\langle x \rangle_t$ in Eq. (36), which gives,

$$\langle x \rangle_t^2 = \left(\langle x \rangle_0 + \frac{\langle p \rangle}{m} t \right)^2 = + \frac{\langle p \rangle^2}{m^2} t^2 + 2 \frac{\langle p \rangle x_0}{m} t + \langle x \rangle_0^2. \tag{44}$$

We can calculate the required second moment $\langle x^2 \rangle_t$ in Eq. (42), using the momentum representation as before,

$$\langle x^2 \rangle_t = \int_{-\infty}^{\infty} c^*(p) e^{\imath \omega t} \left(\imath \hbar \frac{\partial}{\partial p} \right)^2 c(p) e^{-\imath \omega t} \, dp = \langle x^2 \rangle_0 + \frac{\langle p^2 \rangle}{m^2} t^2, \tag{45}$$

where the analytically solution provided is obtained by integration by parts under the assumption that $c(p)$ is real, $c(p)^* = c(p)$. One consequence of this assumption is that $x_0 = 0$ and that the wavepacket is maximally compact at $t = 0$. This assumption is sensible in many scenarios, for instance in time-resolved spectroscopies where the pump pulse is optimised to have as little chirp and thus be as short as possible (known as bandwidth limited). Knowing that the $t = 0$ wavepacket is maximally compact, we can define "dispersion" as the rate of change of the mean deviation,

$$\frac{\sqrt{\triangle x_t^2 - \triangle x_0^2}}{t} = \frac{1}{t} \sqrt{\frac{\triangle p^2}{m^2} t^2} = \frac{\triangle p}{m}, \tag{46}$$

which shows that the variance increases linearly with time t for a wavepacket that is maximally compact at $t = 0$. It is worth noting that this agrees with a classical picture. If we consider $c(p)$ to be a distibution of the momenta in a swarm of classical particles, we do expect that the slowest particles will lag behind the fastest, thus increasing the width of the wavepacket with time.

We can also, as we did for the position of the free wavepacket above, relate the current result to general wavemechanics. The general definition of dispersion is,

$$\text{dispersion} = \frac{\sqrt{\triangle x_t^2 - \triangle x_0^2}}{t} = \left\langle \left(\frac{\partial \omega}{\partial k} \right)^2 \right\rangle - \left\langle \frac{\partial \omega}{\partial k} \right\rangle^2. \tag{47}$$

For the free particle Schrödinger equation $\omega(k) = \hbar k^2 / 2m$, and we find that the dispersion becomes $\triangle p / m$ in agreement with our derivation above.

F. Example: Gaussian wavepackets

Gaussian functions have many attractive mathematical properties, which make them highly used across physics and chemistry: Gaussian basis sets dominate electronic structure calculations, Gaussian wavepackets are used to simulate semiclassical and quantum nuclear dynamics or even electron dynamics, and coherent states are used extensively in quantum optics. In Eq. (30) we defined a general free particle wavepacket with $c(p)$ an arbitrary distribution of momenta. We will now examine the special case where the momentum distribution is a Gaussian function, resulting in a Gaussian wavepacket in both coordinate and momentum representations. We will first investigate the properties of the Gaussian wavepacket for a free particle, and then examine the behaviour of the wavepacket in a quadratic potential.

All of the mathematics for the Gaussian wavepacket can be done analytically, this is part of the attraction, but in order to keep this text reasonably compact we only look at the results here. The interested reader is referred to for instance David Tannor's book *Introduction to quantum mechanics: A time-dependent perspective* [6], which dedicates an entire chapter to Gaussian wavepackets, reflecting their frequent usage in modern molecular quantum dynamics simulation methods. The general form

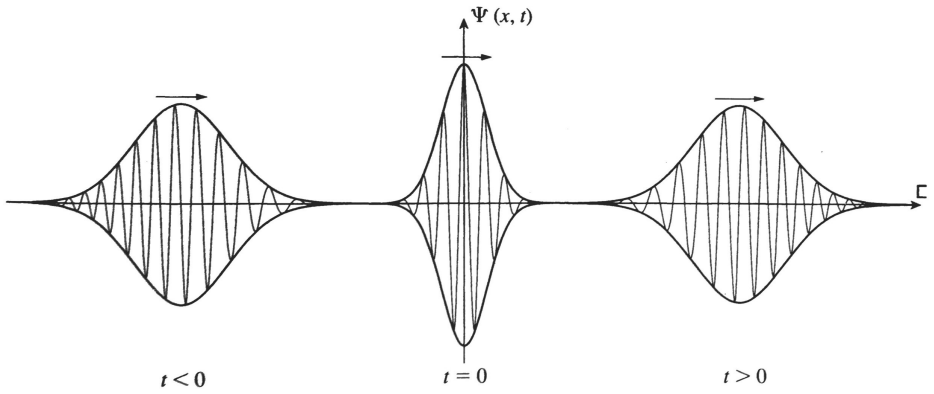

FIG. 6: Time evolution free-particle Gaussian wavepacket. The envelope is the absolute value and the oscillatory curve in the interior is the real part of the wavepacket. The spacing between the oscillations is the measure of the average momentum. The central momentum is constant in time, while the central position changes at a uniform rate, $\langle x\rangle = \langle p\rangle_t t/m$. The width of the packet decreases until $t = 0$ and then increases: at $t = 0$ the wavepacket is a minimum uncertainty state, $\triangle x \triangle p = \hbar/2$, while at earlier and later times $\triangle x \triangle p > \hbar/2$. This is in accordance with the derivation in Section I E 4 above when $c(p)$ is a real-valued function. Note that the height of the wavepacket changes in time in opposition to the width such that the norm is conserved. Taken from D. Tannor *Quantum Mechanics*.

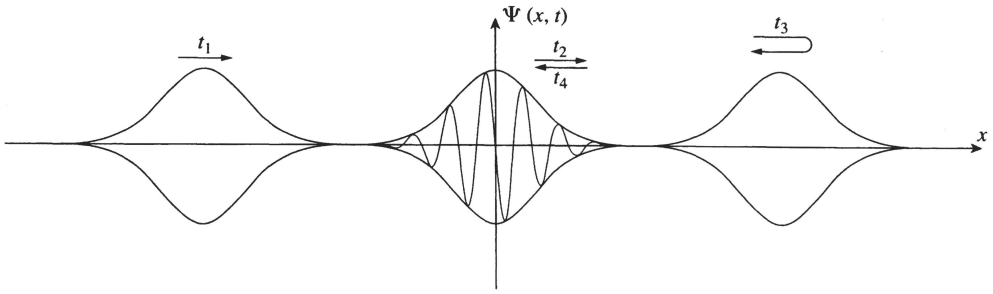

FIG. 7: Gaussian wavepacket (coherent state) in quadratic potential. The envelope is the absolute value and the oscillatory curve in the interior is the imaginary part of the wavepacket. Note that the average position and momentum change according to the classical equations of motion: the average momentum vanishes at the classical turning points and is maximum at the potential minimum. The initial width is the same as the width of the ground vibrational state of the oscillator: $\alpha_0 = m\omega/2\hbar$, where ω is the angular frequency of the oscillator. This is a so-called coherent state, where the Gaussian moves without spreading: $\alpha_t = \alpha_0$. Taken from D. Tannor *Quantum Mechanics*.

mathematical form of a Gaussian wavepacket is,

$$|\Psi(x)\rangle = Ne^{-\alpha(x-x')^2+\imath p'(x-x')/\hbar+\imath\gamma/\hbar}, \tag{48}$$

where α, x', p', and γ are parameters that do not depend on x, but may depend on the time t. We assume that x' and p' are real, while α and γ may be complex. For complex γ the normalisation constant N takes the general form $N = \left(\frac{2\Re\alpha}{\pi}\right)^{1/4} e^{\Im\gamma/\hbar}$. The behaviour of a free-particle Gaussian wavepacket is illustrated in Fig. 6, while the behaviour of a Gaussian wavepacket in a quadratic potential is shown in Figs. 7 - 8. Fig. 7 shows the special case, also known as a coherent state, which occurs when the width of the Gaussian matches the quadratic potential $\alpha_0 = m\omega/2\hbar$, where ω is the angular frequency of the oscillator. In this case the shape of Gaussian wavepacket remains fix at all times, $\alpha_t = \alpha_0$. Fig. 8 shows the more general situations when either $\alpha_0 < m\omega/2\hbar$ or $\alpha_0 > m\omega/2\hbar$. In both these situations the width of the Gaussian wavepacket depends on the position in the quadratic potential.

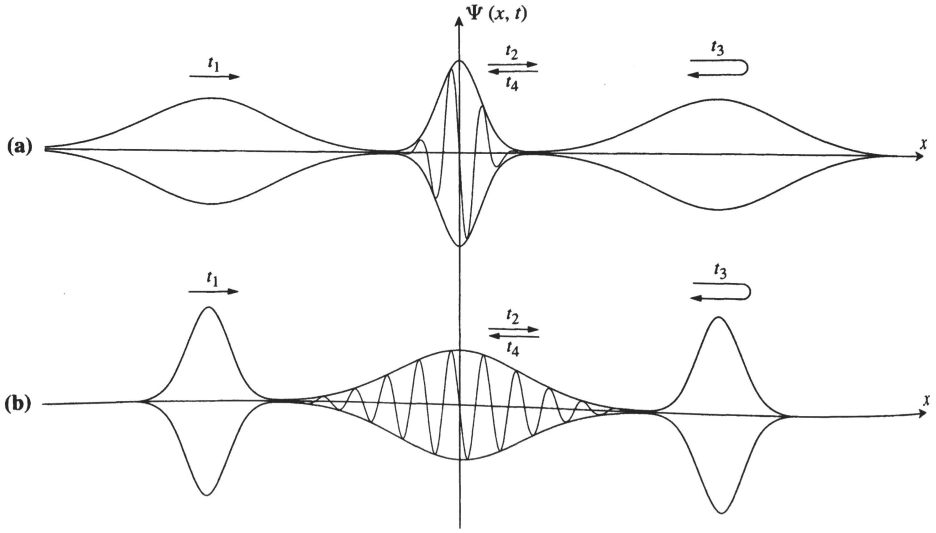

FIG. 8: Gaussian wavepackets (not coherent states) in quadratic potentials, as in Fig. 7, but with a) $\alpha_0 < m\omega/2\hbar$, b) $\alpha_0 > m\omega/2\hbar$. Taken from D. Tannor *Quantum Mechanics*.

G. Flux and stationary states

The probability density is defined as $\rho(\mathbf{x}, t) = |\Psi(\mathbf{x}, t)|^2$. Using the Schrödinger time-dependent equation (see e.g. Sakurai p. 101) one may derive the continuity equation,

$$\frac{\partial \rho}{\partial t} + \nabla \cdot \mathbf{j} = 0, \tag{49}$$

where $\mathbf{j}(\mathbf{x}, t)$ is the probability flux given by,

$$\mathbf{j}(\mathbf{x}, t) = -\frac{\imath\hbar}{2m}\left[\Psi^*\nabla\Psi - (\nabla\Psi^*)\Psi\right] = \frac{\hbar}{m}\Im\left(\Psi^*\nabla\Psi\right). \tag{50}$$

We have already used Eq. (49) to calculate the flux for the particle in a box wavepacket in Fig. 5, corresponding to the wavepacket depicted in Fig. 4. But what about stationary states? It is fair to ask if dynamics is really absent from the stationary solutions. A stationary solution can always taken to be real-valued, meaning that the (net) flux by definition must be zero according to Eq. (49). However, real-valued stationary solutions can be written as a superposition of non-stationary complex solutions.

Consider that the stationary solution to the particle in a box problem can be written as a superposition of $e^{\imath k_n x}$ and $e^{-\imath k_n x}$. Calculating the flux for wavefunctions of the form $e^{\pm\imath k_n x}$, using Eq. (49), we see that the flux for each of the imaginary components is proportional to $\pm k_n$ (Problem III 6). Hence, the absence of flux in the stationary solutions can be seen as coming from a cancellation of opposing fluxes. The stationary nature of these solution is not due to an absence of dynamics *per se*, but due to finely balanced cancellation of fluxes that prevents any net changes in the probability density.

H. Spectra and autocorrelation

We have already mentioned that the range of bound and continuum solutions to a Hamiltonian constitute its spectrum. For a bound wavepacket,

$$|\Psi\rangle = \sum_i c_i e^{-\imath\omega_i t}|i\rangle, \tag{51}$$

the corresponding spectrum $\sigma(\omega)$ is given by,

$$\sigma(\omega) = \sum_i |c_i|^2 \sigma(\omega - \omega_i), \tag{52}$$

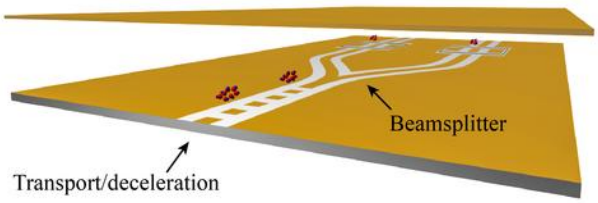

FIG. 9: Micromachined *lab on chip* are currently explored to slow down and trap atoms and molecules for high-resolution spectroscopy, controlled reactions, and quantum computing. Illustration from Prof. Stephen Hogan (UCL); this particular design uses Stark deceleration to slow down the atom/molecule beam.

where $\omega_i = E_i/\hbar$, as before. The spectrum is simply the sum of the weights of the energy components, positioned at the eigenvalue energies. It can be computed from the Fourier transform of the wavepacket autocorrelation function $\langle\Psi(0)|\Psi\rangle$, i.e. the overlap of the wavepacket at any time t with itself at $t = 0$,

$$\sigma(\omega) = \frac{1}{2\pi}\int_{-\infty}^{\infty}\langle\Psi(0)|\Psi(t)\rangle e^{\imath\omega t}\,dt, \tag{53}$$

$$= \frac{1}{2\pi}\int_{-\infty}^{\infty}\left(\sum_i c_i^*\langle i|\right)\left(\sum_j c_j e^{\imath\omega_j t}|j\rangle\right)e^{\imath\omega t}\,dt, \tag{54}$$

$$= \frac{1}{2\pi}\int_{-\infty}^{\infty}\left(\sum_{i,j} c_i^* c_j e^{\imath\omega_j t}\delta_{ij}\right)e^{\imath\omega t}\,dt, \tag{55}$$

$$= \sum_i |c_i|^2\left\{\frac{1}{2\pi}\int_{-\infty}^{\infty} e^{\imath(\omega-\omega_j)t}\,dt\right\}, \tag{56}$$

$$= \sum_i |c_i|^2\delta(\omega-\omega_j). \tag{57}$$

This is a far reaching result, with implications for any kind of measurement or spectroscopy, and it underpins the time-energy uncertainty relation, $\Delta E\Delta t \geq \hbar$. As a consequence, we see that the longer the measurement, the higher the (energy) resolution. For instance in high resolution spectroscopy and metrology, one current trend is to trap and cool atoms or molecules in order to achieve higher accuracy, since slow-moving particles can be measured for longer. Figure 9 shows an illustration of a lab on a chip setup where a micromachined track for atoms or molecules is combined with Stark deceleration to slow them down. Conversely, one draw-back of ultafast measurements is that the short light-pulses inherently limit the energy resolution (although one might still achieve high energy resolution in the detection of the signal itself: time-resolved photoelectron spectroscopy is a good example).

Hence, if a state has a limited lifetime, a measurement of that state will have an inherent spectral width. This width is not due to a failure or shortcoming in the measurement, but a fundamental property of the state. Consider for instance a state that decays exponentially,

$$I(t) = e^{-\Gamma|t|/2}, \tag{58}$$

with half-time $t_{1/2} = 2\ln 2/\Gamma$. The corresponding spectrum of the state, given by the Fourier transform, is

$$\sigma_{\rm L}(\omega) = \mathrm{F}\left[e^{-\Gamma|t|/2}\right](\omega) = \frac{1}{2\pi}\int_{-\infty}^{\infty} e^{-\Gamma|t|/2}e^{\imath\omega t}\,dt = \frac{1}{\pi}\frac{\frac{1}{2}\Gamma}{\omega^2+\left(\frac{1}{2}\Gamma\right)^2}, \tag{59}$$

which is a normalised Lorentzian function centered at $\omega = 0$ with Γ the full width at half maximum (FWHM). Importantly, the width Γ is a *fundamental* width of the state, and even an experiment with perfect resolution cannot achieve a sharper peak. The derivation of the time-energy Fourier transforms between the Lorentzian and exponential decay are given as problems below (Problem III 7 and Problem III 8).

The relationship in Eq. (52) also underpins the original suggestion by Eric Heller [7] that in some circumstances it may be numerically more efficient to solve the TD-SE rather than the time-independent SE (see discussion in Section I A). Instead of solving for multidimensional, difficult to calculate, nuclear eigenstates, one might instead propagate a wavepacket for a limited period of time, which is computationally cheaper and has fewer problems with the handling of boundary conditions. One then calculates the autocorrelation function for the wavepacket, performs a Fourier transform, and obtains the spectrum

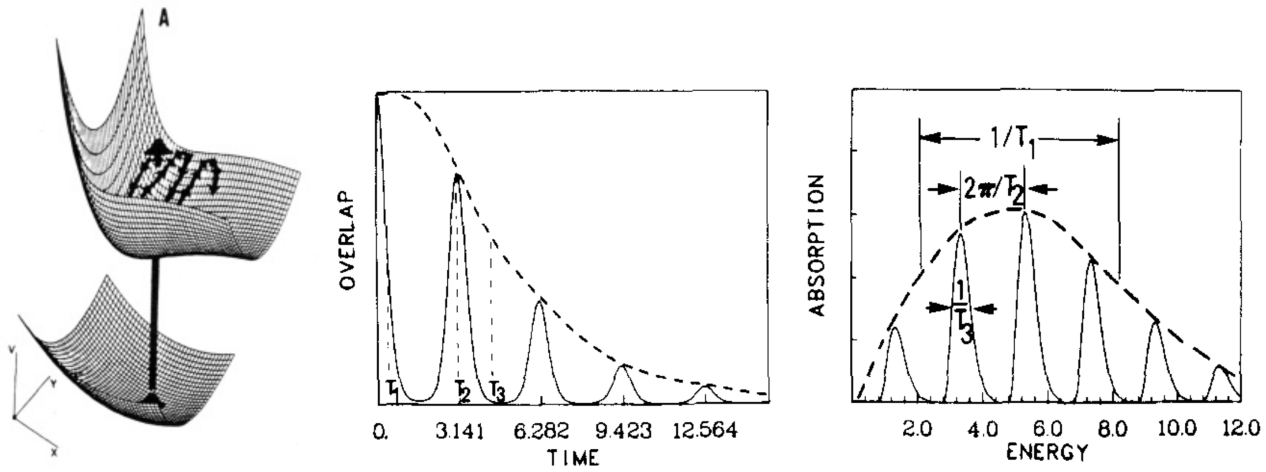

(a) Excited wavepacket dynamics

(b) Autocorrelation (left) and spectrum (right)

FIG. 10: Wavepacket, its autocorrelation, and spectrum. Taken from E. Heller [7].

of eigenvalues. Although the overall resolution will be limited by the total propagation time, most theoretical calculations are compared to experiments with limited resolution anyway. This suggestion had great influence on the direction of computations and theory for decades.

Figure 10 (center panel) shows a typical example of a wavepacket correlation function, corresponding to the situation in Figure 10a where a wavepacket has been excited from the ground state onto an excited Born-Oppenheimer potential energy surface. The wavepacket $|\Psi(0)\rangle = \mu\chi$, arises via Franck-Condon vertical excitation from the ground state χ, then evolves across the potential enerrgy surface, grazing the $|\Psi(0)\rangle$ several times on the way to dissociation. The result is an absorption band with some low-resolution vibrational structure. The absolute value of the autocorrelation function for this wavepacket is shown on the left-hand side of Figure 10b (i.e. in the central panel) with three important time scales, T_1, T_2, and T_3 indicated. The corresponding spectrum (Fourier transform of the autocorrelation function) is shown on the right-hand side, with the effect of the times T_1, T_2, and T_3 indicated. The shortest time T_1 corresponds to the fast initial decay of the autocorrelation of the wavepacket, when the wavepacket initially moves away from the Franck-Condon region. This gives rise to a broad envelope $1/T_1$ in the spectrum (recall that sharp features in time will correspond to broad features in energy). The wavepacket returns to the Franck-Condon region with an approximate period of T_2, leading to recurrences in the autocorrelation function ('fractional revivals'). These recurrences in the time-domain, give a corresponding series of recurrences in the energy domain, with a spacing $2\pi/T_2$. Finally, the long-time decay of the autocorrelation function due to the wavepacket dispersing across different degrees of freedom in the molecule or perhaps photodissociating, gives rise to the width $1/T_3$ of each individual peak in the spectrum. It is important to appreciate that all these effects are straightforward manifestations of the properties of Fourier transforms, and as such are general. In summary:

1. Sharp features in time become broad features in energy, and vice versa.

2. Decay (lifetime) in the time domain become width in the energy domain.

3. Recurrences in the time domain become recurrences in the energy domain.

I. Computer lab

In the computer lab, use Matlab to write a simple wavepacket code for the particle in the box that calculates the wavepacket probability distribution, the expectation value of $\hat{x}$, and (optional) the flux as a function of time.

J. Keywords for revision

- Time-independent and time-dependent Schrödinger equation
- Wavefunctions and wavepackets

- Revivals and fractional revivals
- Normalisation (bound, continuum), norm and probability distribution
- Momentum space representation
- Gaussian wavepackets and coherent states
- Spectrum, autocorrelation and lifetime
- Flux and dynamics in stationary states

II. LIGHT-MATTER INTERACTION

A. Photoexcitation

The quantum dynamics in the presence of an electromagnetic field is given by the time-dependent Schrödinger equation,

$$\imath\hbar\frac{d}{dt}|\Psi(t)\rangle = (H_0 - d\epsilon(t))|\Psi(t)\rangle, \tag{60}$$

where H_0 is the field-free molecular Hamiltonian and the light-matter interaction is given as the product of the time-dependent electromagnetic field $\epsilon(t)$ and the electric dipole operator d ($d = er$). The separation of the dipole operator and the field constitutes the dipole approximation, which is valid only if the dimensions of the absorbing state of the molecule are small compared to the wave length of the light.

Solutions to Equation (59) can be expanded in the complete basis of orthonormal eigenfunctions $|\Psi_i\rangle$ of the Hamiltonian H_0,

$$|\Psi(t)\rangle = \sum_n c_n(t)e^{-\imath E_n t/\hbar}|n\rangle, \tag{61}$$

where E_n is the energy corresponding to state $|n\rangle$ and $c_n(t)$ is a time-dependent expansion coefficient. By substituting this ansatz into the Schrödinger equation and by using the orthonormality of the basis functions, $c_n(t) = \langle n|\Psi(t)\rangle$, we obtain a set of ordinary differential equations for each coefficient $c_m(t)$,

$$\dot{c}_m(t) = \frac{1}{\imath\hbar}\sum_n c_n(t)e^{\imath\omega_{mn}t}d_{mn}\epsilon(t), \tag{62}$$

where $d_{mn} = \langle m|d|n\rangle$ and $\omega_{mn} = (E_m - E_n)/\hbar$. Equation (61) can be integrated numerically, without any assumptions about the intensity of the field.

B. First order perturbation theory

If the perturbation caused by the field is sufficiently weak, we can solve Equation (61) perturbatively to first order. Weak perturbation gives

$$\dot{c}_m^{(1)}(t) = \frac{1}{\imath\hbar}\sum_n c_n^{(0)}e^{\imath\omega_{mn}t}d_{mn}\epsilon(t). \tag{63}$$

Inserting in Equation (62) the initial state $c_i^{(0)} = 1$ (with $c_j^{(0)} = 0, j \neq i$) gives

$$\dot{c}_m(t) = \frac{d_{mi}}{\imath\hbar}e^{\imath\omega_{mi}t}\epsilon(t) \tag{64}$$

which can be integrated in order to obtain the

$$c_m(t) = \frac{d_{mi}}{\imath\hbar}\mathbf{cef}(\omega_{mi}, t) \tag{65}$$

where $\mathbf{cef}(\omega_{mi}, t)$ is obtained as

$$\mathbf{cef}(\omega_{mi}, t) = \int_{-\infty}^{t} dt'\ e^{\imath\omega_{mi}t'}\epsilon(t') = \int_{-\infty}^{\infty} d\omega\ \epsilon(\omega)\int_{T=-\infty}^{t} dt'\ e^{\imath(\omega_{mi}-\omega)t'}, \tag{66}$$

where $\epsilon(\omega)$ is the Fourier transform of $\epsilon(t)$. Note that a real pulse $\epsilon(t)$ requires that $\epsilon(-\omega) = \epsilon^*(\omega)$. For times $t \to \infty$, the integral over t' in Equation (65) becomes $2\pi\delta(\omega_{mi} - \omega)$ and the complex excitation function (abbreviated as CEF) approaches the Fourier limit, $\mathbf{cef}(\omega_{mi}, t \to \infty) = 2\pi\epsilon(\omega_{mi})$.

In a more general case, still within weak field perturbation theory, there are multiple initial states $c_i^{(0)}$. Integration then gives the solution

$$c_m(t) = \frac{1}{\imath\hbar}\sum_j c_j^{(0)}d_{mj}\mathbf{cef}(\omega_{mj}, t) \tag{67}$$

which is a coherent sum of CEF's. The long time limit is

$$c_m(t \to \infty) = \frac{2\pi}{\imath\hbar} \sum_j c_j^{(0)} d_{mj} \epsilon(\omega_{mj}) \tag{68}$$

C. General perturbation theory

We want to solve the time-dependent Schrödinger equation,

$$\imath\hbar \frac{d}{dt} |\Psi(t)\rangle = H(t)|\Psi(t)\rangle, \tag{69}$$

perturbatively. We write the Hamiltonian as

$$H = H_0 + \lambda H'(t), \tag{70}$$

while our ansatz for the wave function is

$$|\Psi(t)\rangle = = \sum_{q=0} \lambda^q |\Psi^{(q)}(t)\rangle |\Psi^{(0)}(t)\rangle + \lambda |\Psi^{(1)}(t)\rangle + \lambda^2 |\Psi^{(2)}(t)\rangle \ldots \tag{71}$$

$$|\Psi^{(q)}(t)\rangle = \sum_i c_i^{(q)}(t)|i\rangle e^{-\imath E_i t/\hbar}, \tag{72}$$

where $|i\rangle$ are eigenstates of the molecular Hamiltonian H_0. Inserting the perturbation ansatz for the wave function and the perturbative Hamiltonian into Equation (68), multiplying by $\langle n|$ on the left and collecting equal powers of λ leads to the following relation

$$\dot{c}_n^{(q)}(t) = \frac{1}{\imath\hbar} \sum_i c_n^{(q-1)}(t)\, e^{\imath\omega_{ni}t} H'_{ni}(t), \tag{73}$$

where $\omega_{ni} = (E_n - E_i)/\hbar$ and $H'_{ni}(t) = \langle n|H'(t)|i\rangle$. It follows immediately that

$$q = 0 \dot{c}_n^{(0)}(t) = 0 \quad \to \quad c_n^{(0)} = \text{constant} \tag{74}$$

$$q = 1 \dot{c}_n^{(1)}(t) = \frac{1}{\imath\hbar} \sum_i c_i^{(0)} e^{\imath\omega_{ni}t} H'_{ni}(t) \tag{75}$$

$$q = 2 \dot{c}_n^{(2)}(t) = \frac{1}{\imath\hbar} \sum_i c_i^{(1)}(t) e^{\imath\omega_{ni}t} H'_{ni}(t). \tag{76}$$

We see that the *constant* zeroth order coefficients $c_n^{(0)}$ give the initial conditions, while all higher order coefficients are zero before the perturbation begins. We also notice that perturbations of successive order are very similar in structure (for $q \geq 1$). This immediately tells us that we can treat successive pulses, which do not overlap temporally, as successive first order perbations. This is an aspect we will exploit in Section III 1. Let us now return to Equations (73-75). The case $q = 0$ is trivial, while integration of the case $q = 1$ proceeds exactly as previously (in Section II B) to give

$$c_n^{(1)}(t) = \frac{1}{\imath\hbar} \sum_i \int_{t_0}^{t} dt' \; c_i^{(0)} e^{\imath\omega_{ni}t'} H'_{ni}(t'). \tag{77}$$

Similarly, integration of the $q = 2$ equation gives

$$c_n^{(2)}(t) = \frac{1}{\imath\hbar} \sum_i \int_{t_0}^{t} dt' \; c_i^{(1)}(t') e^{\imath\omega_{ni}t'} H'_{ni}(t'). \tag{78}$$

Inserting Equation (76) in Equation (77) then produces

$$c_n^{(2)}(t) = \left(\frac{1}{\imath\hbar}\right)^2 \sum_i \sum_j \int_{t_0}^{t} \int_{t_0}^{t'} dt' dt'' \; e^{\imath\omega_{ni}t'} H'_{ni}(t') e^{\imath\omega_{ij}t''} H'_{ij}(t'') c_j^{(0)}. \tag{79}$$

This equation is identical to Equation (13.27) in Tannor's book, except for obvious differences in notation due to differences in the derivation. According to Equation (71) the coefficient $c_n^{(2)}$ must be multiplied by a phase factor $e^{-\imath E_n t/\hbar}$. Performing this multiplication, and rewriting the phase terms in Equation (78) using $\omega_{ij} = (E_i - E_j)/\hbar$, gives an overall phase factor,

$$\text{phase} \propto \quad -E_n(t - t') - E_i(t' - t'') - E_j t''. \tag{80}$$

This Equation lends itself to an attractive interpretation, where we initially accumulate phase on the initial state E_j, until a time t'' when we make a transition to state E_i. We then accumulate phase on this state until a time t', at which we make a transition to the final state E_n, where we make the final phase accumulation from time t' to time t. Of course, in Equation (78) we integrate over all possible transition times t' and t'', and sum over all possibke paths from the initial to the final state.

Finally, from the structure of Equation (72) we see that when the optical field is composed of sequential pulses with no temporal overlap, each pulse will be correctly described by a complex excitation function. This emphasizes that the complex excitation function describes a single-photon process.

D. Case study: Photodissociation from single state

E. Weak field

We will now investigate photodissociation (or equivalently, photoionization) from a single initial state i, and take the opportunity to introduce incoming state, which are the appropriate boundary conditions to use. The following results are derived in the weak field regime, but will later show that similar results can be derived beyond the weak field. A continuum wave packet can be written as

$$|\Psi(t)\rangle = \frac{1}{\imath\hbar} \sum_n^{N_o} \int dE \; d_{ni}^-(E) \mathbf{cef}(\omega_{Ei}, t) e^{-\imath E t/\hbar} |n^-(E)\rangle, \tag{81}$$

where we have assumed $c_i = 1$ for the initial state and the sum runs over the N_o open channels. The incoming (-) state boundary conditions and the corresponding incoming states $|n^-(E)\rangle$, are appropriate when $t \to \infty$ properties are required. Each $|n^-(E)\rangle$ state evolves in the *distant future* to a well defined state of the separated fragments $|n^0(E)\rangle$. More precisely we have that

$$\lim_{t\to\infty} \langle m^0(E')|n^-(E)\rangle = \delta_{n,m}\delta(E - E') \tag{82}$$

If we assume that the incoming states are orthogonal, i.e. $\langle n^-(E')|m^-(E)\rangle = \delta_{nm}\delta(E' - E)$ and $\langle n^-(E)|i\rangle = 0$, we can isolate each component of the wave packet by projection

$$\langle n^-(E')|\Psi(t)\rangle = \frac{d_{ni}^-(E')}{\imath\hbar} \mathbf{cef}(\omega_{E'i}, t) \; e^{-\imath E' t/\hbar}. \tag{83}$$

The probability for each channel is then obtained via the asymptotic amplitude of the state $e^{-\imath E t/\hbar}|n^-(E)\rangle$ at $t \to \infty$ is

$$A_n(E|i) = \lim_{t\to\infty} e^{\imath E t/\hbar} \langle n^-(E)|\Psi(t)\rangle = \frac{2\pi}{\imath\hbar} d_{ni}^-(E)\epsilon(\omega_{Ei}) \tag{84}$$

which gives the probability

$$P_n(E|i) = |A_n(E|i)|^2 = \frac{4\pi^2}{\hbar^2} |\epsilon(\omega_{Ei})|^2 |d_{ni}^-(E)|^2. \tag{85}$$

The probability $P_n(E|i)$ in Equation (84) is the probability per unit energy of observing a given asymptotic channel (when exciting from initial state i with the field $\epsilon(\omega_{Ei})$ in the weak field approximation). From Equation (84) we see that there is no phase effect and that $P_n(E|i)$ is only proportional to transition and pulse intensities. We also find that the cross section is independent of the pulse;

$$\sigma_n(E|i) = \frac{\hbar\omega_{Ei} P_n(E|i)}{I(E)} = \frac{4\pi^2 \omega_{Ei} |d_{ni}^-(E)|^2}{c} \tag{86}$$

where $I(E) = |\epsilon(E)|^2 c/\hbar$. Hence the cross section is independent of the pulse (see also Brumer and Shapiro p. 28). The energy integrated probability is

$$P_{ni} = \int dE\ P_n(E|i) \tag{87}$$

and the ratio between different channels is

$$R_{nm} = \frac{P_n}{P_m} = \frac{\int dE\ |\epsilon(\omega)|^2 |d^-_{ni}(E)|^2}{\int dE\ |\epsilon(\omega)|^2 |d^-_{mi}(E)|^2} \tag{88}$$

Note that the pulse envelope can change the ratio, but the phase has no effect on the branching ratio.

To do: show the following

$$P_n = \int_0^\infty dt\ flux_n(t) \tag{89}$$

F. Comparison between pulse and CW excitation

In many experiments the product translational energy is not well defined. Under these circumstances one might argue that the energetic profile imparted to the molecule by the laser pulse may substantially modify the relative yields. The relevant quantity here is the integral over the laser profile

$$P_m = \int dE\ |d^-_{mi}(E)|^2 |\epsilon(E)|^2. \tag{90}$$

Two extreme limits may be compared, a high resolution cw experiment and a broadband short pulse excitation.

A high resolution experiment is one in which the laser frequency profile is substantially narrower than the relevant molecular feature. This means $d^-_{mi}(E)$ is slowly varying across the laser profile, and we obtain that

$$P_m = |d^-_{mi}(E)|^2 f_L(E_L), \tag{91}$$

where $f_L(E_L)$ is the radiative energy density integrated over the laser profile

$$f_L(E_L) = \int dE\ |\epsilon(E)|^2 \tag{92}$$

and E_L is the energetic center of the laser line. If the experiment is repeated by varying E_L over the molecular spectral feature, each time irradating with a narrow band laser whose integrated energy $f_L(E_L)$ is allowed to change with E_L, one obtains the average yield to a specific channel as

$$Y_m = \frac{\int dE_L\ |d^-_{mi}(E)|^2 f_L(E_L)}{\sum_n \int dE_L\ |d^-_{ni}(E)|^2 f_L(E_L)}. \tag{93}$$

Inspection of Equation (90) shows that this is *precisely* the yield obtained by irradiating the sample with a *single* coherent pulse with a shape given by function $f_L(E_L)$.

The most intriguing aspect of this present derivation is the fact that although the time dependence of the dissociative wave packet created in the two experiments is drastically different, the average yield to the various *asymptotic* product channels remains the same. The relative yield of any given channel is inherent in the stationary scattering states and although the short pulse excitation may create an almost pure local state at $t = 0$, the fate of this local state is the same as that of the integrated yield obtained by successively exciting nearly stationary scattering statas. Thus, shaping a single laser pulse cannot improve yields or funnel products ti desired channels beyond what is attainable in a related collection of cw experiments. For further material on this section, see [8**?** , 9].

G. Strong field

Does the result in Section II E change if we go beyond perturbation theory? Following the ansatz in Equation (60), a general continuum wave packet is given by

$$|\Psi(t)\rangle = \sum_{n}^{N_o} \int dE\ c_{nE}(t) e^{-\imath Et/\hbar} |n^-(E)\rangle \tag{94}$$

assuming the same orthogonality relations as above. This gives

$$\langle n^-(E')|\Psi(t)\rangle = c_{nE'}(t)\ e^{-\imath E' t/\hbar}. \tag{95}$$

With only one initial state i and no intermediate states, integration gives

$$c_{nE}(t) = \frac{d^-_{ni}(E)}{\imath\hbar} \int_{-\infty}^{t} dt'\ \epsilon(t') e^{-\imath\omega_{Ei}t'} c_i(t') \tag{96}$$

The branching ratio hence becomes

$$R_{nm}(E) = \frac{P_n(E)}{P_m(E)} = \left|\frac{c_{nE}(t\to\infty)}{c_{nE}(t\to\infty)}\right|^2 = \left|\frac{d^-_{ni}(E)}{d^-_{mi}(E)}\right|^2 \tag{97}$$

and as in the weak field case the branching ratio is independent of the pulse. This result is valid provided that the material Hamiltonian does not cause substantial coupling between the radiation modes. This is usually the case with single photon dissociation/ionization experiments. This result is not valid for multiphoton transitions.

H. Case study: Photodissociation from superposition state

When the initial state is

$$|\chi(t)\rangle = \sum_{j=1}^{N_j} c_j |j\rangle e^{-\imath E_j t/\hbar}, \tag{98}$$

where N_j is the number of states in the initial superposition state $|\chi(t)\rangle$, the continuum wave packet becomes (within perturbation theory)

$$|\Psi(t)\rangle = |\chi(t)\rangle + \frac{1}{\imath\hbar} \sum_{j}^{N_j} c_j \sum_{n}^{N_o} \int dE\ d^-_{nj}(E) \mathbf{cef}(\omega_{Ej}, t) e^{-\imath Et/\hbar} |n^-(E)\rangle, \tag{99}$$

where N_o is the number of open channels and N_j is the number of states in the initial state superposition. We assume, as before, that $\langle n^-(E')|m^-(E)\rangle = \delta_{nm}\delta(E'-E)$ and $\langle n^-(E)|j\rangle = 0$. The projection on each open channel at energy E becomes

$$\langle n^-(E)|\Psi(t)\rangle = \frac{1}{\imath\hbar} \sum_{j}^{N_j} c_j\, d^-_{nj}(E) \mathbf{cef}(\omega_{Ej}, t)\ e^{-\imath Et/\hbar} \tag{100}$$

The amplitude of state $e^{-\imath Et/\hbar}|n^-(E)\rangle$ at $t\to\infty$ is

$$A_n(E) = \lim_{t\to\infty} \frac{2\pi}{\imath\hbar} \sum_{j}^{N_j} c_j\, d^-_{nj}(E) \epsilon(\omega_{Ej}) \tag{101}$$

which gives the probability

$$P_n(E) = |A_n(E)|^2 = \frac{4\pi^2}{\hbar^2} \left| \sum_{j}^{N_j} c_j d^-_{nj}(E) \epsilon(\omega_{Ej}) \right|^2 \tag{102}$$

The branching ratio becomes

$$R_{nm}(E) = \frac{min[P_n(E)]}{max[P_m(E)]} \leq \frac{P_n(E)}{P_m(E)} \leq \frac{max[P_n(E)]}{min[P_m(E)]} \tag{103}$$

As before, the actual ratio will be an integral over energy

$$R_{nm} = \frac{\int dE\ P_n(E)}{\int dE\ P_m(E)} \tag{104}$$

I. Case study: Photodissociation by two pulses

1. No temporal overlap between pulses

The following is a discussion of photodissociation by two optical pulses with no temporal overlap in the weak field (i.e. we can use sequential first order perturbation theory). Assume we have a sequence of two pulses, one excitation pulse $\epsilon_x(t)$ and one dissociation pulse $\epsilon_d(t)$. The total pulse is

$$\epsilon(t) = \epsilon_x(t - t_1) + \epsilon_d(t - t_2), \tag{105}$$

where the pulses are centered at times t_x and t_d respectively and the delay between the two pulses is $\Delta t = t_d - t_x$. The ansatz for the solution can be written as

$$|\Psi(t)\rangle = c_i(t)e^{-\imath E_i t/\hbar}|i\rangle + \sum_j^{N_j} c_j(t)e^{-\imath E_j t/\hbar}|j\rangle + \sum_n^{N_o} \int dE\ c_{En}(t)e^{-\imath E_n t/\hbar}|n^-(E)\rangle, \tag{106}$$

where $|i\rangle$ is the initial state, the states $|j\rangle$ are intermediate discrete states and $|n^-(E)\rangle$ are incoming continuum states. We will solve the time dependent Schrödinger equation using perturbation theory.

We examine three (mutually non-exclusive) scenarios, shown in Figure 11. The first scenario, shown in Figure 11a, corresponds to the initial state being connected to (the intermediate) manifold of states by the rotating wave contribution part of each of the two consecutive pulses. This scenario can be treated as follows. Assuming the initial state is $c_0 = 1$ and applying Equation (63), we obtain

$$c_m(t) = \frac{d_{mi}}{\imath\hbar}\mathbf{cef}(\omega_{mi}, t) \tag{107}$$

where, according to Equation (65) we have

$$\mathbf{cef}(\omega_{mi}, t) = \mathbf{cef}_x(\omega_{mi}, t) + \mathbf{cef}_d(\omega_{mi}, t) \tag{108}$$

with the long time limit

$$\mathbf{cef}(\omega_{mi}, t \to \infty) = 2\pi\epsilon_x(\omega_{mi}) + 2\pi\epsilon_d(\omega_{mi}). \tag{109}$$

This gives the expansion coefficients in Equation (105) as

$$c_i(t) = 1 \tag{110}$$

$$c_j(t) = (2\pi/\imath\hbar)[\epsilon_x(\omega_{j0}) + \epsilon_d(\omega_{j0})]d_{j0} \tag{111}$$

$$c_{En}(t) = 0, \tag{112}$$

where we have assumed that before the first pulse initial conditions are that $c_0 = 1$. For two identical time-delayed pulses $\epsilon_x = \epsilon_d$ this gives an interference term directly proportional to the time delay Δt, which we can see of we rewrite Equation (110) as,

$$c_j(t) = (2\pi/\imath\hbar)\left[2|\epsilon|\cos\omega_{j0}\Delta t/2\right]d_{j0}, \tag{113}$$

where we have used that $\epsilon_x = |\epsilon|e^{\imath\omega_{j0}t_x}$, $\epsilon_d = |\epsilon|e^{\imath\omega_{j0}t_d}$, and $\Delta t = t_x - t_d$.

The second scenario, depicted in Figure 11b is somewhat different, because it involves a set of intermediate states, which allow for multiple pathways for excitation to a final energy E. This scenario can either be solved formally exactly by entering

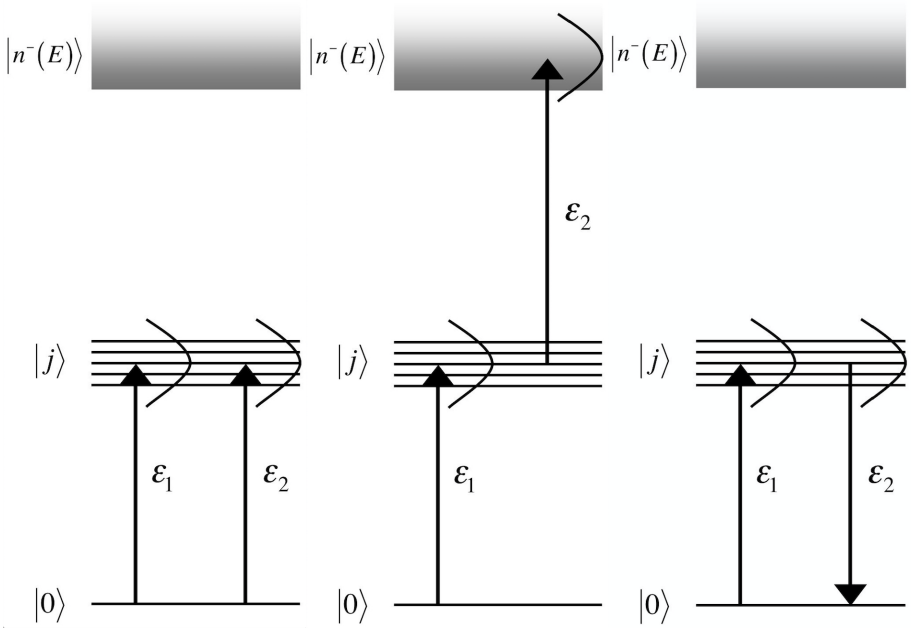

(a) Two pulses, excitation only from the initial state, rotating wave contribution from both pulses.

(b) Two pulses, excitation from intermediate states by rotating wave contribution from secondpulse.

(c) Two pulses, counter rotating wave contribution from second pulse.

FIG. 11: The various scenarios for excitation with a sequence of pulses, with initial boundary condition $c_0(t = -\infty) = 1$. Note that the scenarios are not mutually exclusive and that $|0\rangle = |i\rangle$.

the pulse sequence given by Equation (104) into the Schrödinger Equation (61), which can then be solved numerically, or by a two-step perturbative approach, which works because the two pulses are temporally separated. In Section II I 2 we will see how this assumption can be lifted by second order perturbation theory. After the excitation pulse ϵ_x, but before the dissociation pulse ϵ_d, first order perturbation theory gives the expansion coefficients in Equation (105) as

$$c_i(t) = 1 \tag{114}$$
$$c_j(t) = (2\pi/\imath\hbar)\epsilon_x(\omega_{j0})d_{j0} \tag{115}$$
$$c_{En}(t) = 0 \tag{116}$$

where again we have assumed that before the first pulse initial conditions are that $c_0 = 1$. First order perturbation theory gives for the dissociation pulse that

$$c_0(t) = 1 \tag{117}$$
$$c_j(t) = (2\pi/\imath\hbar)\epsilon_x(\omega_{j0})d_{j0} \tag{118}$$
$$c_{En}(t) = \frac{2\pi}{\imath\hbar}\sum_j^{N_j} c_j d^-_{nj}(E)\epsilon_d(\omega_{Ej}) \tag{119}$$

Since the two pulses are temporally separated, we can set the values of c_j to the values obtained in Equation (114), which gives

$$c_{En}(t \to \infty) = \left(\frac{2\pi}{\imath\hbar}\right)^2 \sum_j^{N_j} d_{j0}d^-_{nj}(E)\epsilon_x(\omega_{j0})\epsilon_d(\omega_{Ej}). \tag{120}$$

In doing so, we have to pay attention to the phase evolution of the coefficients of the intermediate states between the two pulses (i.e. during the time delay Δt). This evolution can either be included explicitly in the coefficients, or follows from the general properties of the Fourier transform of the two pulses. A linear shift in time gives a corresponding shift in phase in the Fourier transform, $f(t - t_0) \leftrightarrow e^{\imath\omega t_0}F(\omega)$. Hence, the Fourier transforms of the excitation and the dissociation pulse will have the frequency dependent phase factors $\exp(\imath\omega_{j0}t_x)$ and $\exp(\imath\omega_{Ej}t_d)$ respectively. We make all the phases explicit by the following

relations

$$\epsilon_x(\omega_{j0}) = |\epsilon_x(\omega_{j0})| \exp\left[\imath\alpha_x(\omega_{j0}) + \imath\omega_{j0}t_x\right] \tag{121}$$

$$\epsilon_d(\omega_{Ej}) = |\epsilon_d(\omega_{Ej})| \exp\left[\imath\alpha_d(\omega_{Ej}) + \imath\omega_{Ej}t_d\right] \tag{122}$$

$$d^-_{nj}(E) = |d^-_{nj}(E)| \exp\left[\imath\alpha^-_{nj}(E)\right]. \tag{123}$$

Inserting these relations in Equations (120) and (119) gives

$$c_{En}(t \to \infty) = e^{\imath\alpha_0(E)} \left(\frac{2\pi}{\imath\hbar}\right)^2 \sum_j^{N_j} |r_j| e^{\imath \arg(r_j)} \tag{124}$$

$$|r_j| = |d_{j0} d^-_{nj}(E) \epsilon_x(\omega_{j0}) \epsilon_d(\omega_{Ej})| \tag{125}$$

$$\arg(r_j) = \alpha^-_{nj}(E) + \alpha_x(\omega_{j0}) + \alpha_d(\omega_{Ej}) - E_j\Delta t/\hbar \tag{126}$$

where we used that $\omega_{ij} = (E_i - E_j)/\hbar$. The pre-sum phase factor $\exp \imath\alpha(E)$, with $\alpha_0(E) = (Et_d - E_0 t_x)/\hbar$, has no physical consequences and disappears when we calculate probabilities. The factor $E_j\Delta t/\hbar$ is the time evolution of the coefficients of the intermediate states between the first and the second pulse. Note that the only channel specific phase comes from the $\alpha^-_{nj}(E)$ term.

The third case, in Figure 11c, is obtained by using the counter rotating wave contribution from the second pulse (the two previous cases only use the rotating wave contribution for both pulses). Finally, as in previous sections, the probability is,

$$P_n(E) = |c_{En}|^2 \tag{127}$$

and

$$P_n = \int dE\ P_n(E) \tag{128}$$

2. Allowing for temporal overlap between pulses

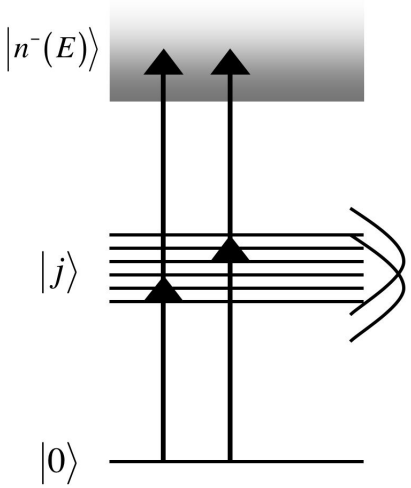

FIG. 12: Two pulse time-domain control is equivalent to two vs. two photon control in the frequency domain, where control is achieved through the interference of multiple two photon routes between the initial and final states.

When we investigate photodissociation induced by two (weak-field) pulses without the assumption of no temporal overlap we must use second order perturbation theory. All that is required, really, is to apply Equation (78) from Section II C, which we reproduce here for convenience.

$$c^{(2)}_n(t) = \left(\frac{1}{\imath\hbar}\right)^2 \sum_i \sum_j \int_{t_0}^{t} \int_{t_0}^{t'} dt' dt''\ e^{\imath\omega_{ni}t'} H'_{ni}(t') e^{\imath\omega_{ij}t''} H'_{ij}(t'') c^{(0)}_j. \tag{129}$$

Note that $H'_{ij} = d_{ij}\mathbf{cef}(\omega_{ij}, t)$ in the present context. Equation (128) lends itself (correctly) to a time-independent interpretation of two pulse control as a case of two vs. two photon control (see Figure 12).

Numerically, it is most convenient to solve each order of perturbation in succession, following the Equations

$$q = 0\dot{c}_n^{(0)}(t) = 0 \quad \rightarrow \quad c_n^{(0)} = \text{constant} \tag{130}$$

$$q = 1\dot{c}_n^{(1)}(t) = \frac{1}{\imath\hbar}\sum_i c_i^{(0)} e^{\imath\omega_{ni}t} H'_{ni}(t) \tag{131}$$

$$q = 2\dot{c}_n^{(2)}(t) = \frac{1}{\imath\hbar}\sum_i c_i^{(1)}(t) e^{\imath\omega_{ni}t} H'_{ni}(t), \tag{132}$$

where Equation (129) are the initial conditions, Equation (130) is the first order contribution, and in solving Equation (131) we make use of the first order solution already obtained, and etc for higher orders.

3. Phase-locking

The three different scenarios according to Figure 11 put different demands on the phase-locking of the two pulses. The two scenarios in Figures 11b and 11c, which correspond to classical pump-pump or pump-dump, do *not* depend on phase-locking. This is can be seen as follows. Allow each of the two pulses acquire some constant phase; δ_x for the excitation pulse and δ_d for the dissociation pulse. Since these phase factors are constant, they can be collected in the pre-sum phase factor, $\exp \imath\alpha(E)$, in Equation (123). The phase factor simply becomes $\alpha_0(E) = \delta_x + \delta_d + (Et_d - E_0 t_x)/\hbar$, and as before, it has no physical consequences and disappears. Hence, phase-locking between the two pulses is not required. Perhaps more intuitive is to consider that during excitation, all intermediate states are given the *same* phase-kick δ_x, and similarly during the second pulse, all states are given the same phase δ_d. Clearly, this simply amounts to a global phase-shift, which has no effect on the interference (control).

The first scenario, show in Figure 11a, is somewhat different. In this case we have an optical interference (see Equation (110), where we have a sum of the fields, rather than a product). Adding a constant phase factor δ_x and δ_d to the excitation and dissociation pulses respectively, will clearly change the interference term. Especially in the case of two identical pulses, we find that Equation (112) becomes

$$c_j(t) = (2\pi/\imath\hbar)\left[2|\epsilon|\cos\omega_{j0}\Delta t/2 + \delta_x - \delta_d\right] d_{j0}. \tag{133}$$

Hence, in this scenario, phase-locking of the two pulses *is* required, since the phase difference $\delta_x - \delta_d$ enters the interference term.

Another situation where phase-locking becomes important is bichromatic control, where two different lasers connect a two-state, non-degenerate, initial superposition state with a final energy E. The two lasers have the angular frequency ω_{E1} and ω_{E2} respectively. Here the control depends on the relative phase of the two lasers, which clearly must be phase-locked in order for control to be meaningful.

III. PROBLEMS

1. Separation of variables for TD-SE

Illustrate the separation of variables for the time-dependent Schrödinger equation by assuming that $|\Psi\rangle = \theta(t)|i\rangle$, where $\theta(t)$ is a function of time to be determined and $|i\rangle$ is an eigenstate of the time-independent Schrödinger equation [Eq. (1)].

2. Norm of wavepacket

Using the orthonormality of the stationary wavefunctions, show that the norm of a wavepacket is preserved.

3. Momentum space representation

Derive the momentum p representation of particle in a box wavefunctions given by Eq. (23), i.e. solve the integral on the left-hand side,

$$\frac{1}{\sqrt{2\pi\hbar}}\int_{-\infty}^{\infty}\Psi_n(x)e^{-\imath px/\hbar}\,dx = \sqrt{\frac{\hbar}{\pi L}}\left(\frac{p_n}{p_n^2-p^2}\right)\left[1-(-1)^n e^{-\imath pL/\hbar}\right] = \tilde{\Psi}_n(p).$$

4. Normalisation of momentum space wavepacket

Show that given a normalised coordinate wavepacket the norm of the corresponding momentum space wavepacket is also conserved.

5. Variance

Show that $\mathrm{Var}(x) = \langle (x-\langle x\rangle)^2\rangle = \langle x^2\rangle - \langle x\rangle^2$.

6. Flux

Calculate the flux corresponding to a free particle eigenstate,

$$\Psi(x) = \frac{1}{\sqrt{2\pi\hbar}}e^{\pm\imath p' x/\hbar}.$$

7. FT of exponential decay

Show that the Fourier transform of an exponential decay is a Lorentzian function, $\sigma_{\mathrm{L}}(\omega)$, i.e. solve,

$$\sigma_{\mathrm{L}}(\omega) = \mathrm{F}\left[e^{-\Gamma|t|/2}\right](\omega) = \frac{1}{2\pi}\int_{-\infty}^{\infty} e^{-\Gamma|t|/2}e^{\imath\omega t}\,dt.$$

8. FT of Lorentzian peak

In this problem we practice our skills in integration by doing the opposite Fourier transform to that in Problem III 7 by transforming a Lorentzian spectral peak,

$$\sigma_{\mathrm{L}}(\omega) = \frac{1}{\pi} \frac{\frac{1}{2}\Gamma}{\omega^2 + \left(\frac{1}{2}\Gamma\right)^2}, \tag{134}$$

to the time domain. To get from the energy domain to the time domian we require the inverse Fourier transform compared to Problem III 7,

$$\mathrm{F}\left[\sigma_{\mathrm{L}}(\omega)\right](t) = \int_{-\infty}^{\infty} \sigma_{\mathrm{L}}(\omega) e^{-\imath\omega t}\, d\omega.$$

Note that we have adopted the convention that the Fourier transform carries the entire prefactor $(2\pi)^{-1}$, which means that the inverse Fourier transform has no prefactor at all. This is in contrast to our symmetric definition of the Fourier transform between coordinate and momentum states, where each direction carries a $(2\pi)^{-1/2}$ prefactor.

IV. COURSE INFORMATION

A. Further reading

Although it is hard to find a single book that reflects these notes, the following books cover much of the material (and more): *Physics of atoms and molecules* by B. H. Bransden and C. J. Joachain [10], *Molecular Quantum Mechanics* by P. W. Atkins [11], *Quantum Mechanics* by C. Cohen-Tannoudji, B. Diu, and F. Laloë [12], *Quantum Mechanics* by J. J. Sakurai [13], and *Introduction to Quantum Mechanics: A Time-Dependent Perspective* by D. J. Tannor [6].

B. Future developments

The ambition is to extend this course with new sections (lectures) every year with the ultimate goal of a complete set of lectures covering a wide range of topics in chemical physics from the theory perspective. Topics under development include:

- Molecules:
  - Molecular Hamiltonians, separation of variables, Born-Oppenheimer approximation, and the derivation of close-coupled equations (mainly for the case of diatomics).
  - Scattering collisions, cross-sections, and resonances
  - Electron collisions (diffraction of high-energy electrons and electron-molecule scattering
  - Rydberg atoms/molecules (introduction to MQDT)
  - Autoionisation and photoionisation
- More on light-matter interaction:
  - Perturbative and non-perturbative regime (Keldysh parameter, multiphoton perturbative regime and strong-field regime including NSDI and HHG)
  - Scattering of light
  - Feynman diagrams
  - Coherent control

---

[1] Yuan T. Lee. Nobel lecture: Molecular beam studies of elementary chemical processes, 2014. Nobelprize.org. Nobel Media AB 2014.
[2] M. S. Child. *Molecular Collision Theory*. Dover Publications Inc., new edition (21 april 1997) edition, 1997.
[3] Eric J. Heller. The semiclassical way to molecular spectroscopy. *Acc. Chem. Res.*, 14(12):368, 1981.
[4] Examples of grid based integration methods include Runge-Kutta, renormalized Numerov, and the logderivative method, but in many cases methods that exploit grids of basis functions instead of spatial grids are preferrable, for instance in electronic structure theory, both *ab-initio* and density functional theory (DFT).
[5] In fact, in one of the computer labs we will use a code called *Wavepacket* that does exactly this.
[6] David J. Tannor. *Introduction to Quantum Mechanics: a time-dependent perspective*. University Science Books, 2007.
[7] Eric J. Heller. Frozen Gaussians: A very simple semiclassical approximation. *J. Chem. Phys.*, 75(6):2923, Sep 1981.
[8] Moshe Shapiro and Paul Brumer. The equivalence of unimolecular decay product yields in pulsed and cw radiation. *J. Chem. Phys.*, 84:540, 1986.
[9] Moshe Shapiro and Paul Brumer. *Faraday Discuss.*, 1986.
[10] B. H. Bransden and C. J. Joachain. *Physics of atoms and molecules*. Addison Wesley Longman Limited, first edition, 1983.
[11] P. W. Atkins. *Molecular Quantum Mechanics*. Oxford University Press, second edition, 1983.
[12] Cohen-Tannoudji, Diu, and Laloe. *Quantum Mechanics*. J. Wiley and Sons, 1977.
[13] J. J. Sakurai. *Modern Quantum Mechanics*. Addison-Wesley Publishing Company, 1994.